

## Photodegradation and durability of LPNTP-promoted N-doped TiO<sub>2</sub> in a continuous-flow photocatalysis/membrane separation system

Hsu-Hui. Cheng<sup>a,c,\*</sup>, Shiao-Shing Chen<sup>b</sup>, Yi-Wen Cheng<sup>b</sup>, Sih-Yin Yang<sup>a,c</sup>,  
Shih-Jie Chou<sup>b</sup>, Hung-Te Hsu<sup>d</sup>

<sup>a</sup>Department of Landscape Architecture and Environmental Planning, Mingdao University, 369, Wen-Hua Rd, Peetow, Changhua 52345, Taiwan, ROC, email: hhcheng1126@gmail.com (H.-H. Cheng)

<sup>b</sup>Institute of Environment Engineering and Management, National Taipei University of Technology, 1, Sec.3 Chung-Hsiao E. Rd., Taipei 10643, Taiwan, ROC, email: f10919@ntut.edu.tw (S.-S. Chen), ywen6697@gmail.com (Y.-W. Cheng), b037325533@gmail.com (S.-J. Chou)

<sup>c</sup>Hsuteng Consulting Technology Co., Ltd. No.11, Ln. 42, Fukang Rd., Xitun Dist., Taichung City 40764, Taiwan, ROC, email: lovey1124@gmail.com (S.-Y. Yang)

<sup>d</sup>Department of Environmental Engineering, Chung Yuan Christian University, No. 200, Chung Pei Rd, Chung Li District, Taoyuan City 32023, Taiwan, ROC, email: der11065@hotmail.com (H.-T. Hsu)

### ABSTRACT

Yellow N-doped TiO<sub>2</sub> (TiO<sub>x</sub>N<sub>y</sub>) powder, synthesized using the liquid-phase nonthermal plasma technique, was produced from a mixed aqueous solution containing commercial titanium dioxide (Degussa P-25) and an N-precursor (ammonium chloride, NH<sub>4</sub>Cl), and used for photodegrading C. I. Acid Orange 7 (AO7) in a continuous-flow photocatalysis–membrane separation system. The effects of the initial AO7 concentration, TiO<sub>x</sub>N<sub>y</sub> dose, oxygen concentration, and solution pH on AO7 photodegradation were investigated to obtain the optimum operational conditions. The experimental results indicate that the optimal dose of TiO<sub>x</sub>N<sub>y</sub> was 0.5 g L<sup>-1</sup>, and the AO7 degradation efficiency was effectively improved by increasing the oxygen concentration from 0% to 40% or reducing the initial AO7 concentration from 15 to 5 mg L<sup>-1</sup>. Moreover, the degradation efficiency for AO7 increased as pH decreased, with the catalyst exhibiting maximum efficiency at pH 2. The durability of the photocatalyst was evaluated by reusing the photocatalyst 11 times, and the recycled catalyst could repeat five runs without a significant decrease in treatment efficiency. In addition, the durability of the TiO<sub>x</sub>N<sub>y</sub> catalysts with aeration, which reduces catalyst deactivation, was longer than that without aeration.

*Keywords:* Photodegradation; Durability; N-doped TiO<sub>2</sub>; LPNTP technique

### 1. Introduction

The textile industry has played a major role in Taiwan's economic development, but the textile processing industry consumes a large amount of water through its various processing operations. Wastewater from textile dyeing is characterized by deep color, high oxygen demand, high pH, large amounts of suspended solids, and low biodegradability or nonbiodegradability [1,2], and the release of this colored wastewater into the environment causes a serious ecological

problem. At present, several conventional methods are used to treat textile dye wastewater, such as Fenton oxidation [3], coagulation–flocculation [4], biological treatment and membrane filtration [5], and activated carbon adsorption [4,6]. However, these methods still generate a tremendous amount of sludge or solid waste, which requires further treatment.

Recently, an increase in the application of advanced oxidation processes to industrial wastewater has been observed. Among these processes, TiO<sub>2</sub> heterogeneous photocatalysis is a very promising technique for wastewater treatment [7], especially for wastewater containing refractory organic compounds. The photocatalytic degradation

\*Corresponding author.

Presented at the 6th IWA-ASPIRE Conference & Exhibition, Beijing, China, 20–24 September 2015.

process has several advantages, such as complete mineralization, effective disposal of waste solids, low cost, and the capability to operate in mild temperature and mild pressure conditions [8–12]. However, the band gap of pure  $\text{TiO}_2$  for the anatase crystalline phase is 3.2 eV; thus, it can absorb solar light only in the near ultraviolet (UV) region [13,14]. Therefore, the development of  $\text{TiO}_2$  photocatalysts with high efficiency under visible-light irradiation is crucial to ensuring its practicality and widespread use. Many studies have been conducted to enhance the visible-light sensitization of  $\text{TiO}_2$ . Among the viable doping elements or compounds for  $\text{TiO}_2$ , the substitutional doping of nitrogen has long been recognized as one of the most effective means of producing visible and solar light irradiation effects [15]. Consequently, applying N-doped  $\text{TiO}_2$  ( $\text{TiO}_x\text{N}_y$ ) for removing various types of organic pollutants from the environment, such as acetaldehyde, methylcyclohexene, benzoic acid, phenol, and methyl orange (MO), has recently been reported [16]. Notwithstanding the substantial advantages of  $\text{TiO}_x\text{N}_y$  for photocatalytic degradation, this technique has yet to be implemented in the large-scale treatment of industrial wastewater. The main problem is the lack of suitable hardware, namely a large catalyst surface area per unit volume of reactor.

Currently, immobilized and suspended systems are the most common applications of photoreactor configurations [17]. For a  $\text{TiO}_x\text{N}_y$ -immobilized system, the limited catalyst surface area and poor diffusive transportation are major drawbacks, even though the immobilization obviates filtration requirements [18,19]. However, the  $\text{TiO}_x\text{N}_y$ -suspended system can provide a higher surface area for adsorption and reaction, but the finely dispersed  $\text{TiO}_x\text{N}_y$  powder is difficult to separate, recover, and reuse from the liquid phase [20,21].

In our previous study [22], we successfully used liquid-phase nonthermal plasma (LPNTP) to prepare  $\text{TiO}_x\text{N}_y$  photocatalysts, combining a ceramic UF membrane to recover the  $\text{TiO}_x\text{N}_y$  powder in the suspension system. However, the effect of various operating parameters on the photocatalytic degradation of Acid Orange 7 (AO7) dyes in the photoreactor with continuous flow was not described. Furthermore, the activity of the photocatalyst could decrease over time because of factors such as surface masking and catalyst poisoning [11], but very few studies have discussed the relationship between catalyst lifetime and catalyst activity.

Therefore, the aim of the present study was to determine the photocatalytic degradation of AO7 dyes over a visible-light illuminated  $\text{TiO}_x\text{N}_y$  catalyst in a continuous-flow photocatalysis–membrane separation system (PMSS) and to examine the effect of operational parameters, such as the initial concentration,  $\text{TiO}_x\text{N}_y$  dose, solution pH, and oxygen concentration. In addition, the durability of the  $\text{TiO}_x\text{N}_y$  catalyst was evaluated through recycling experiments.

## 2. Materials and methods

### 2.1. Experimental setup

The experimental setup was a continuous-flow PMSS system, as shown in Fig. 1. The continuous-flow photocatalytic reactor was composed of two quartz reactor tubes in one unit. The two quartz tubes had a 30-mm inside diameter (length: 250 mm) and were symmetrically installed inside the photocatalytic reactor, with an effective volume of 700 mL, and the outside of the reactor was coated in tinfoil to increase the efficiency of visible

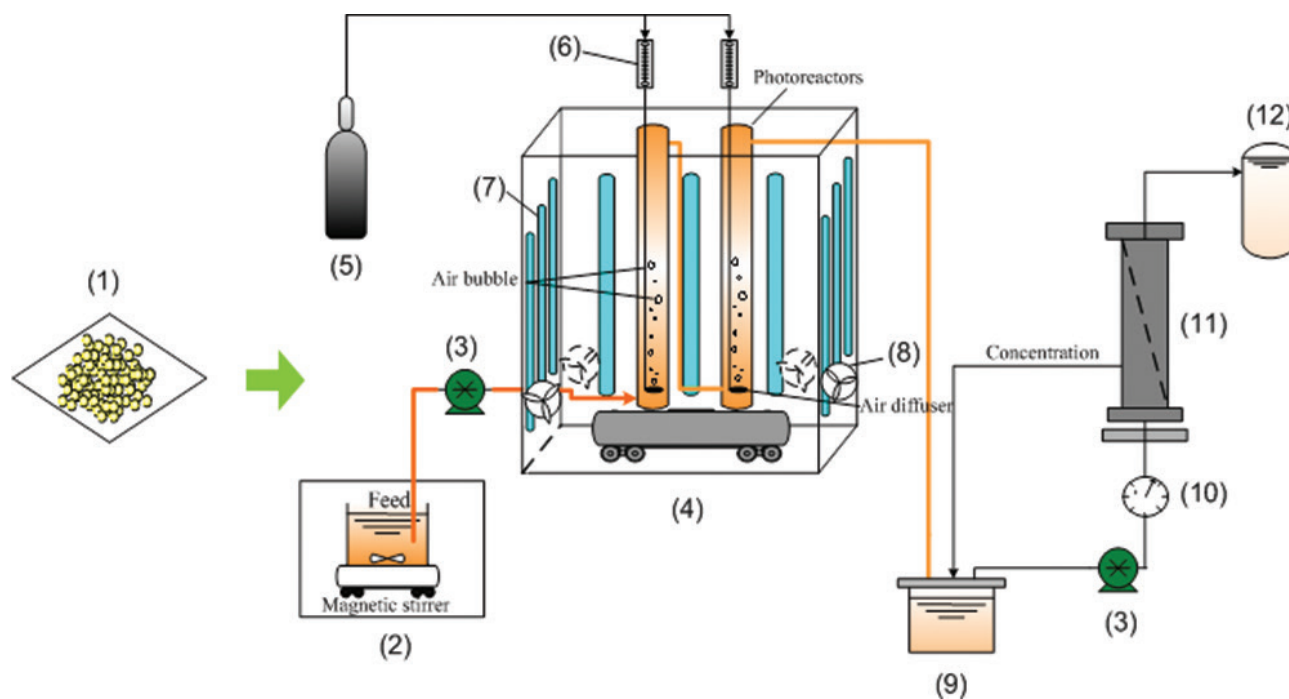


Fig. 1. Main elements of the continuous-flow PMSS: (1) preparing the  $\text{TiO}_x\text{N}_y$  photocatalyst; (2) feed tank ( $V_a = 2$  L); (3) pump; (4) photocatalytic reactor; (5) gas cylinder; (6) flow meter; (7) visible light ( $I_{\max} = 419$  nm); (8) fan; (9) feed tank ( $V_b = 3$  L); (10) manometer (0–4 bar); (11) ceramic UF membranes; (12) permeate tank; schematic drawing of the up-flow fluidized bed system.

light irradiation. The photoreactor was surrounded by 12 light tubes in total. The visible-light tubes were germicidal lamps with a wavelength of 419 nm (Sankyo Denki Co., Ltd.). The light power in the air at the center of the reactor was approximately 10 mW cm<sup>-2</sup>, measured by a power meter (Model 840-C, Handheld). A gas diffuser from a gas cylinder was placed at the bottom of the quartz tube reactor. The stirring speed was as high as 600 rpm to ensure the complete mixing of liquid and gas phases, consistent with previous tests. The ceramic membrane separation system comprised a 3-L feed tank, where the photodegraded AO7 solution was circulated at a constant speed by a circulating pump operated with a cross-flow module. The ceramic membrane tube was manufactured by Pall Membrane Co. USA (Membralox® T1-70) with a length of 250 mm, outer diameter of 10 mm, and inner diameter of 7 mm. The membrane was composed of a selective layer of zirconia with a pore size of 10 nm on an  $\alpha$ -alumina porous support. The membrane total surface area was 0.005 m<sup>2</sup>. The transmembrane pressure was 2.8 bar, the temperature was 25°C, and the cross-flow velocity was 0.0001 m s<sup>-1</sup>. The experimental procedure was as follows. Two liters of the reacting mixture were prepared by suspending the desired amounts of TiO<sub>x</sub>N<sub>y</sub> catalyst in distilled water containing a certain amount of AO7 dye. The suspension was first stirred in the dark for 30 min before irradiation, and this was sufficient to generate an equilibrium adsorption concentration. The photodegraded AO7 solution was then poured into the 3-L feed tank through the ceramic membrane tube to recover the catalyst in the separation system.

## 2.2. Preparation of TiO<sub>x</sub>N<sub>y</sub>

Yellow TiO<sub>x</sub>N<sub>y</sub> powder, which was synthesized through the LPNTP technique, was produced from a mixed aqueous solution containing commercial titanium dioxide (Degussa P-25) and an N-precursor of an ammonium chloride (NH<sub>4</sub>Cl) solution. The pH value of the NH<sub>4</sub>Cl solution was adjusted to 5, and the suspended mixture of TiO<sub>2</sub> in the NH<sub>4</sub>Cl solution was transferred to the LPNTP reactor, which was operated at 13.5 W for 40 min. The prepared TiO<sub>x</sub>N<sub>y</sub> powder was then washed with water three times to remove impurities and moved to an oven for continual 3-h desiccation at 573 K. More details of the LPNTP system are described in our previous study [22]. The TiO<sub>x</sub>N<sub>y</sub> particles were prepared under our optimal photocatalyst conditions as TiO<sub>x</sub>N<sub>y</sub>-1:6. The primary particle size, BET surface area, wavelength, and band gap of the TiO<sub>x</sub>N<sub>y</sub> powder are shown in Table 1. AO7 with purity of above 99% was obtained from Tokyo Kasei Kogyo (Japan), and

Table 1  
Particle size, BET surface area, and band gap of photocatalysts

Sample	Particle size (nm)	BET surface area (m <sup>2</sup> /g)	Band gap (eV)	Wavelength (nm)
TiO <sub>x</sub> N <sub>y</sub> -1:6	32	50.18	2.82	439

all the other chemicals that were used were of reagent grade. The photodegradation rates of the AO7 solutions were determined by measuring the absorbance at  $\lambda = 486$  nm periodically by using a Hach DR/4000 UV/VIS spectrophotometer. The concentration of H<sub>2</sub>O<sub>2</sub> was determined through spectrophotometric analysis by using the potassium titanium oxalate method ( $\lambda = 400$  nm) [23].

## 3. Results and discussion

### 3.1. Influence of operational parameters

#### 3.1.1. Effect of initial AO7 concentration and dose of TiO<sub>x</sub>N<sub>y</sub>

The effect of the initial AO7 concentration on the photocatalytic degradation efficiency was examined for different AO7 concentrations from 5 to 15 mg L<sup>-1</sup> under a TiO<sub>x</sub>N<sub>y</sub> dose of 0.15 g L<sup>-1</sup>, hydraulic retention time (HRT) of 10 h, pH of 5, and  $Q_{air}$  of 200 mL min<sup>-1</sup>. Fig. 2(a) shows the AO7 removal efficiency and observed rate constant ( $k_{obs}$ ) as a function of the initial AO7 concentration at a pH of 5 and HRT of 10 h. The photodegradation of AO7 was observed to decrease with an increase in the initial AO7 concentration. When the initial AO7 concentration is increased, more AO7 dye molecules are adsorbed onto the surface of TiO<sub>x</sub>N<sub>y</sub> to prevent light adsorption. Therefore, the photons cannot reach the

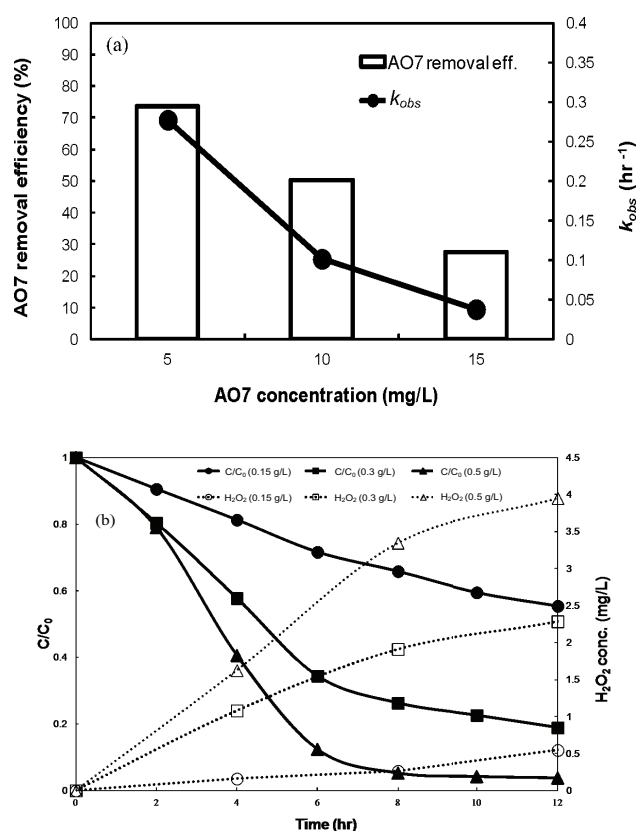


Fig. 2. (a) AO7 removal efficiency and  $k_{obs}$  as a function of the initial concentration (TiO<sub>x</sub>N<sub>y</sub> = 0.15 g L<sup>-1</sup>, HRT = 10 h, pH = 5, and  $Q_{air}$  = 200 mL min<sup>-1</sup>); (b) comparison of the removal efficiency for AO7 and H<sub>2</sub>O<sub>2</sub> generation under different TiO<sub>x</sub>N<sub>y</sub> doses (AO7 = 10 mg L<sup>-1</sup>, HRT = 10 h, pH = 5, and  $Q_{air}$  = 200 mL min<sup>-1</sup>).

photocatalyst surface, and the photodegradation efficiency decreases [24]. Albeoyeh et al. [25] obtained similar results for AO8, AO7, and MO dyes.

In addition, the photocatalytic degradation of the AO7 reached a steady state after 16 h and followed a pseudo-first-order kinetics model. The mass balance equation for the pseudo-first-order kinetics of a continuous-flow reactor can be expressed as follows [26]:

$$dC_{A1} V = C_{A0} Q dt - V k_{obs} C_{A1} dt - C_{A1} Q dt \quad (1)$$

where  $V$  is the reactor volume (L),  $Q$  is the flow rate (L h<sup>-1</sup>),  $C_{A0}$  and  $C_{A1}$  are the initial and effluent AO7 concentrations (mg L<sup>-1</sup>), and  $k_{obs}$  is the observed constant rate of removal (h<sup>-1</sup>). Under steady-state conditions,  $dC_{A1}/dt = 0$ , the HRT is  $T = V/Q$ ; thus, Eq. (1) can be reformulated as follows:

$$\frac{C_{A1}}{C_{A0}} = \frac{1}{1 + k_{obs} T} \quad (2)$$

According to Eq. (2) [26], the reaction rate constants for the initial AO7 concentrations of 5, 10, and 15 mg L<sup>-1</sup> were  $2.77 \times 10^{-1} \text{ h}^{-1}$ ,  $1.02 \times 10^{-1} \text{ h}^{-1}$ , and  $3.80 \times 10^{-2} \text{ h}^{-1}$ , respectively. As displayed in Fig. 2(a),  $k_{obs}$  and AO7 degradation efficiency decrease as the initial AO7 concentration increases. A possible explanation for the decrease in the removal rate is that, as the initial concentration of the dye increases, the path length of the photons entering the solution decreases. Moreover, as mentioned previously, an increase in concentration reduces light penetration; thus, the relative formation of OH radicals and O<sub>2</sub><sup>•-</sup> decreases, reducing the photodegradation efficiency [27].

Additionally, the amount of catalyst is one of the most crucial parameters for degradation analysis from an economic perspective. Fig. 2(b) shows that the degradation efficiencies for 0.15, 0.3, and 0.5 g L<sup>-1</sup> of TiO<sub>x</sub>N<sub>y</sub> were 50.38%, 81.08%, and 96.22%, respectively. Therefore, the optimal dose of TiO<sub>x</sub>N<sub>y</sub> in this continuous-flow photoreactor was determined to be 0.5 g L<sup>-1</sup> because nearly complete reduction of AO7 was achieved in this experimental condition. Furthermore, Fig. 2(b) shows that the generated H<sub>2</sub>O<sub>2</sub> concentrations were 0.71 mg L<sup>-1</sup> for TiO<sub>x</sub>N<sub>y</sub> at 0.15 g L<sup>-1</sup>, 2.78 mg L<sup>-1</sup> for TiO<sub>x</sub>N<sub>y</sub> at 0.3 g L<sup>-1</sup>, and 4.58 mg L<sup>-1</sup> for TiO<sub>x</sub>N<sub>y</sub> at 0.5 g L<sup>-1</sup>. The results indicate that increasing the catalyst loading increased the H<sub>2</sub>O<sub>2</sub> concentration, facilitating reduction of the AO7. Although several studies [28,29] have indicated that H<sub>2</sub>O<sub>2</sub> occurs in the UV light photocatalytic system, the aforementioned result in the present study indicates that the generation of H<sub>2</sub>O<sub>2</sub> was observed in our visible-light photocatalytic system. Therefore, an appropriate dose of TiO<sub>x</sub>N<sub>y</sub> facilitates the generation of H<sub>2</sub>O<sub>2</sub> and increases the photodegradation efficiency.

### 3.1.2. Effect of solution pH

To study the effect of pH on the degradation efficiency, experiments were performed under visible light at pH values from 2 to 11 at a constant AO7 dye concentration and TiO<sub>x</sub>N<sub>y</sub> catalyst loading. The results in Fig. 3(a) indicate that the photodegradation efficiency for AO7 increased as pH decreased, with the catalyst exhibiting maximum efficiency (76%) at pH 2. The degradation rates for the continuous-flow photoreactor system followed the order pH 2 > pH 5 > pH

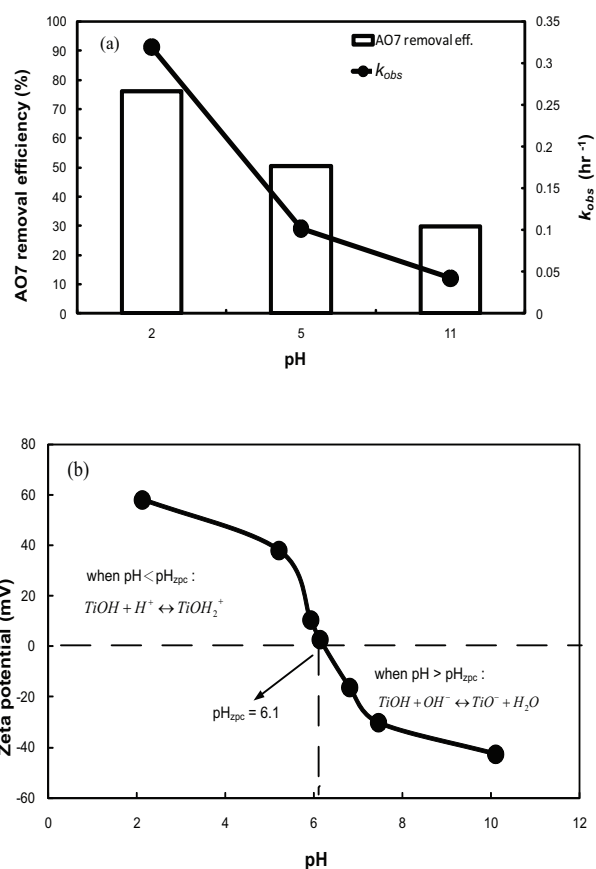
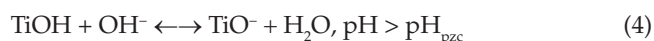
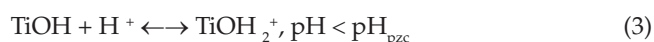


Fig. 3. (a) AO7 removal efficiency and  $k_{obs}$  as a function of pH (AO7 = 10 mg L<sup>-1</sup>, HRT = 10 h, TiO<sub>x</sub>N<sub>y</sub> = 0.15 g L<sup>-1</sup>, and  $Q_{air}$  = 200 mL min<sup>-1</sup>); (b) zeta potential of TiO<sub>x</sub>N<sub>y</sub> particles.

11, and similar observations have been reported by other researchers [30,31]. The effect of pH on the efficiency of dye photodegradation plays multiple roles. First, the pH change is related to the functionalized surface charge of a solid catalyst, according to the following reactions [32]:



With reference to Eq. (3), when TiO<sub>2</sub> is suspended in an acidic solution (pH < point of zero charge, pH<sub>pzc</sub>), the surface charge of the TiO<sub>2</sub> becomes positive. However, when TiO<sub>2</sub> is suspended in a basic solution (pH > pH<sub>pzc</sub>), the surface charge becomes negative, as displayed in Eq. (4). From Fig. 3(b), pH<sub>pzc</sub> for the TiO<sub>x</sub>N<sub>y</sub> was measured as 6.1. Therefore, the surface of the catalyst is negatively charged for pH > 6.1 and positively charged for pH < 6.1. Because the AO7 dye used in the present study was an anionic dye and was negatively charged under experimental conditions because of the sulfonate (SO<sub>3</sub><sup>-</sup>) groups, electrostatic interactions between the TiO<sub>x</sub>N<sub>y</sub> photocatalyst and sulfonate groups resulted in adsorption at pH < 6.1 to enhance the deg-



radiation efficiency (Fig. 3(a)). Conversely, adsorption of AO7 onto  $\text{TiO}_x\text{N}_y$  surfaces is weak at  $\text{pH} > 6.1$ , because of Coulombic repulsion between the negatively charged  $\text{TiO}_x\text{N}_y$  and AO7 molecules; thus, the degradation efficiency decreases. At pH values ranging from 5 to 10, the formation of more OH radicals because of the presence of large quantities of OH anions (Eq. (5)) improves the photodegradation efficiency for the AO7 dye. Experimental results indicate that the degradation efficiency at pH 5 exceeded that at pH 11.



### 3.1.3. Effect of oxygen concentration

This section further examines the effect of different oxygen concentrations on the photodegradation of AO7. Experiments were performed under visible light at oxygen concentrations from 0% to 40% for a constant AO7 dye concentration ( $10 \text{ mg L}^{-1}$ ) and  $\text{TiO}_x\text{N}_y$  catalyst dose ( $0.15 \text{ g L}^{-1}$ ), as displayed in Fig. 4(a). The results clearly show that the highest AO7 photodegradation was observed for the concentration of oxygen ( $\text{O}_2 = 40\%$ ), where the AO7 photodegradation achieved 63% removal after 16 h of visible-light illumination. Conversely, the removal efficiency was the lowest at an oxygen concentration of 0%. This was attributed to the adsorption of molecular oxygen onto the surface of the  $\text{TiO}_x\text{N}_y$  photocatalyst, which instantly traps the interfacial electrons of the photocatalyst to suppress hole–electron recombination because of the presence of residual oxygen in the reaction system [33,34]. Consequently, the decomposition rate increases with an increasing oxygen concentration, and these observations are in good agreement with the reports in the literature [35,36].

The results in Fig. 4(b) show that the linear equation between  $k_{\text{obs}}$  and the  $\text{O}_2$  concentration is  $Y_{k_{\text{obs}}} = 0.0032 \times \text{O}_2$  concentration + 0.0292 with  $R^2 = 0.9338$  for oxygen concentrations of 0% to 40%. The mechanism for increasing oxygen to achieve higher removal efficiency is explained as follows: The  $\text{TiO}_x\text{N}_y$  has a new energy band that narrows the band gap; thus, the  $\text{TiO}_x\text{N}_y$  exhibits stronger absorption in the visible-light region and is activated to generate pairs of electron (valance band) holes and conduction bands (CBs) (Eq. (6)) [11]. Subsequently, the electron of the  $\text{TiO}_x\text{N}_y$  particles is scavenged by molecular oxygen to generate superoxide ions ( $\text{O}_2^{\bullet-}$ ) (Eq. (7)) [37], which can produce  $\text{H}_2\text{O}_2$  and OH radical species (Eqs. (8)–(10)) [38]. These active species facilitate photodegradation or mineralization (Eq. (11)) [38].

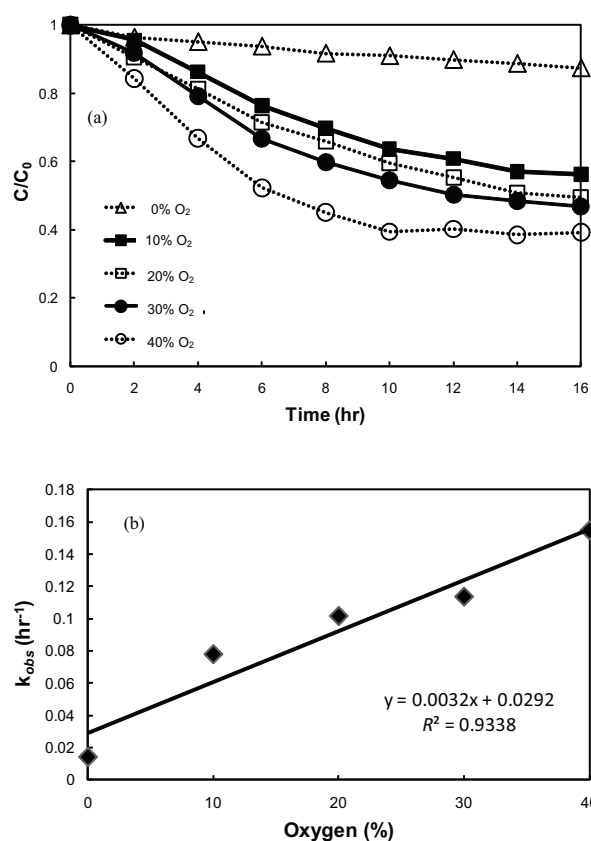
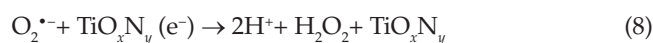
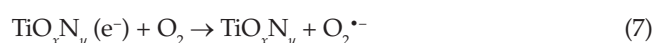


Fig. 4. Effect of different oxygen concentrations: (a) effect of the oxygen concentration on the degradation of AO7 against the illumination time; (b) degradation rate constant ( $k_{\text{obs}}$ ) vs. oxygen percentage plotted on a straight line (AO7 =  $10 \text{ mg L}^{-1}$ , HRT = 10 h,  $\text{TiO}_x\text{N}_y = 0.15 \text{ g L}^{-1}$ ,  $\text{pH} = 5$ , and  $Q_{\text{air}} = 200 \text{ mL min}^{-1}$ ).



Sun et al. [39] indicated that the new absorption band in the visible range originated from the  $\text{TiO}_x\text{N}_y$  particles and the photosensitized oxidation mechanism originated from the azo dyes themselves, contributing to the higher visible-light activity. However, Liu et al. [40] reported on the photodegradation of azo dyes by  $\text{TiO}_x\text{N}_y$  and indicated that the highest occupied molecular orbital and lowest unoccupied molecular orbital of the azo dyes are located in the band gap of  $\text{TiO}_x\text{N}_y$ ; thus, the charge injection mechanisms forming the dyes to photocatalyze CB are not efficient. Consequently, instead of azo dyes, molecular oxygen plays a crucial role in the photo-oxidation of the dyes by LPNTP-promoted  $\text{TiO}_x\text{N}_y$  under visible light.

### 3.2. Durability assessment of $\text{TiO}_x\text{N}_y$ catalyst

To assess the durability of the catalyst, experiments under a  $\text{TiO}_x\text{N}_y$  dose of  $0.15 \text{ g L}^{-1}$ , HRT of 10 h, and pH of 5 were conducted with and without aeration. The

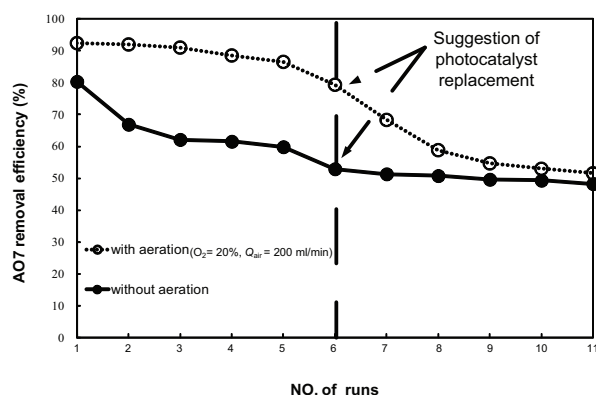


Fig. 5. Durability assessment of the  $\text{TiO}_x\text{N}_y$  catalyst ( $\text{TiO}_x\text{N}_y = 0.15 \text{ g L}^{-1}$ ,  $\text{AO7} = 10 \text{ mg L}^{-1}$ , and  $\text{pH} = 5$ ).

photocatalyst that was separated after each reaction run was washed with reagent-grade water three times, dried at  $120^\circ\text{C}$  for 12 h in an oven, and reused in the subsequent reaction under identical conditions. The results in Fig. 5 show that the removal efficiency for AO7 was as high as 87% after the catalyst was repeatedly used for five runs under aeration conditions; however, the AO7 removal efficiency rapidly decreased from 79% to 58% after six runs. Finally, the AO7 removal efficiency reached a steady-state value of approximately  $53\% \pm 2\%$  after 9–11 runs. Our results clearly indicate that the  $\text{TiO}_x\text{N}_y$  catalyst was recycled through membrane filtration without a decline in flux, and the recycled catalyst was capable of repeating five runs without a significant decrease in the treatment efficiency. However, after six experimental runs, the  $\text{TiO}_x\text{N}_y$  catalyst exhibited a significant decrease in activity. This paper recommends replacing the  $\text{TiO}_x\text{N}_y$  catalyst after six runs of repeated use.

Because aeration reduces catalyst poisoning, the  $\text{TiO}_x\text{N}_y$  catalyst's durability under aeration conditions was determined to be longer than that without aeration. Because molecular oxygen in an aqueous solution plays a critical role as an electron scavenger, trapping the photo-generated electrons from the CB [41] and forming superoxide ions ( $\text{O}_2^{\cdot-}$ ), it delays electron-hole recombination ( $\text{O}_2 + e^- \rightarrow \text{O}_2^{\cdot-}$ ) [42,43] as well as extends the lifetime of the catalyst. Similar results were observed by Janus et al., who reported the lifetime and regeneration of supported carbon-modified  $\text{TiO}_2$  applied in the degradation of Reactive Red 198 (RR 198) dye under UV light in a batch reactor [8]. Their results clearly indicated that the time for RR 198 dye degradation without additional aeration was longer than that with aeration and the carbon-modified  $\text{TiO}_2$  was reused for 10 runs with a decrease in the removal efficiency from 72% to 67%. Kaur and Singh [44] reported that a  $\text{TiO}_2$  photocatalyst was reused for four runs with a decrease in the removal efficiency from 98% to 40%. In our case, the  $\text{TiO}_x\text{N}_y$  catalyst's activity decreased after five runs with aeration and after six runs without aeration. The decrease in the efficiency of the reused catalyst may have been attributable to the deposition of degradation products such as 2-naphthol, 2-hydroxy-1,4-naphthoquinone,

and smaller aromatic intermediates on the photocatalyst surface to block its active sites [11]. These observations closely agree with those of previous studies [44].

#### 4. Conclusions

The photodegradation of the AO7 dye in an aqueous medium by LPNTP-promoted  $\text{TiO}_x\text{N}_y$  under various operating conditions is reported. The AO7 removal efficiency increased from 50.38% for  $\text{TiO}_x\text{N}_y$  at  $0.15 \text{ g L}^{-1}$  to more than 96.22% for  $\text{TiO}_x\text{N}_y$  at  $0.5 \text{ g L}^{-1}$  under visible-light irradiation, and an optimal  $\text{TiO}_x\text{N}_y$  dose of  $0.5 \text{ g L}^{-1}$  was determined. The degradation efficiency for AO7 increased as the pH decreased, with the catalyst exhibiting maximum efficiency at pH 2. The presence of oxygen enhances degradation because of the formation of  $\text{O}_2^{\cdot-}$  and further yields reactive  $\text{OH}^\cdot$ . The durability of  $\text{TiO}_x\text{N}_y$  was evaluated by reusing the photocatalyst 11 times, and the recycled catalyst was capable of repeated use for five runs without a significant decrease in the treatment efficiency. In addition, the durability of the  $\text{TiO}_x\text{N}_y$  catalysts with aeration, which reduces catalyst deactivation, was longer than that without aeration.

#### References

- [1] C.C. Liu, Y.H. Hsieh, P.F. Lai, C.H. Li, C.L. Kao, Photodegradation treatment of azo dye wastewater by UV/ $\text{TiO}_2$  process, *Dyes Pigm.*, 68 (2006) 191–195.
- [2] X. Lu, B. Yang, J. Chen, R. Sun, Treatment of wastewater containing azo dye reactive brilliant red X-3B using sequential ozonation and upflow biological aerated filter process, *J. Hazard. Mater.*, 161 (2009) 241–245.
- [3] İ. Arslan, I.A. Balcioglu, D.W. Bahnemann, Advanced chemical oxidation of reactive dyes in simulated dyehouse effluents by ferrioxalate-Fenton/UV-A and  $\text{TiO}_2$ /UV-A processes, *Dyes Pigm.*, 47 (2000) 207–218.
- [4] F. Harrelkas, A. Azizi, A. Yaacoubi, A. Benhammou, M.N. Pons, Treatment of textile dye effluents using coagulation–flocculation coupled with membrane processes or adsorption on powdered activated carbon, *Desalination*, 235 (2009) 330–339.
- [5] R. Żyła, J. Sójka-Ledakowicz, E. Stelmach, S. Ledakowicz, Coupling of membrane filtration with biological methods for textile wastewater treatment, *Desalination*, 198 (2006) 316–325.
- [6] P.K. Malik, Dye removal from wastewater using activated carbon developed from sawdust: adsorption equilibrium and kinetics, *J. Hazard. Mater.*, 113 (2004) 81–88.
- [7] R. Jothiramalingam, M.K. Wang, Synthesis, characterization and photocatalytic activity of porous manganese oxide doped titania for toluene decomposition, *J. Hazard. Mater.*, 147 (2007) 562–569.
- [8] M. Janus, E. Kusiak, J. Choina, J. Ziebro, A.W. Morawski, Enhanced adsorption of two azo dyes produced by carbon modification of  $\text{TiO}_2$ , *Desalination*, 249 (2009) 359–363.
- [9] J. Luan, S. Wang, K. Ma, Y. Li, B. Pan, Structural property and catalytic activity of new  $\text{In}_2\text{YbSbO}_7$  and  $\text{Gd}_2\text{YbSbO}_7$  nanocatalysts under visible light irradiation, *J. Phys. Chem. C*, 114 (2010) 9398–9407.
- [10] O. Diwald, T.L. Thompson, T. Zubkov, S.D. Walck, J.T. Yates, Photochemical activity of nitrogen-doped rutile  $\text{TiO}_2(110)$  in visible light, *J. Phys. Chem. B*, 108 (2004) 6004–6008.
- [11] I.K. Konstantinou, T.A. Albanis,  $\text{TiO}_2$ -assisted photocatalytic degradation of azo dyes in aqueous solution: kinetic and mechanistic investigations: a review, *Appl. Catal. B*, 49 (2004) 1–14.
- [12] M. Anpo, M. Takeuchi, The design and development of highly reactive titanium oxide photocatalysts operating under visible light irradiation, *J. Catal.*, 216 (2003) 505–516.

- [13] Y. Wang, C. Feng, Z. Jin, J. Zhang, J. Yang, S. Zhang, A novel N-doped TiO<sub>2</sub> with high visible light photocatalytic activity, *J. Mol. Catal. A Chem.*, 260 (2006) 1–3.
- [14] I.C. Kang, Q. Zhang, S. Yin, T. Sato, F. Saito, Novel method for preparation of high visible active N-doped TiO<sub>2</sub> photocatalyst with its grinding in solvent, *Appl. Catal. B*, 84 (2008) 570–576.
- [15] C. Chen, H. Bai, S. Chang, C. Chang, W. Den, Preparation of N-doped TiO<sub>2</sub> photocatalyst by atmospheric pressure plasma process for VOCs decomposition under UV and visible light sources, *J. Nanopart. Res.*, 9 (2007) 365–375.
- [16] J. Ananpattarachai, P. Kajitvichyanukul, S. Seraphin, Visible light absorption ability and photocatalytic oxidation activity of various interstitial N-doped TiO<sub>2</sub> prepared from different nitrogen dopants, *J. Hazard. Mater.*, 168 (2009) 253–261.
- [17] D. Li, K. Xiong, W. Li, Z. Yang, C. Liu, X. Feng, X. Lu, Comparative study in liquid-phase heterogeneous photocatalysis: model for photoreactor scale-up, *Ind. Eng. Chem. Res.*, 49 (2010) 8397–8405.
- [18] S.P. Kamble, S.B. Sawant, V.G. Pangarkar, Photocatalytic degradation of m-dinitrobenzene by illuminated TiO<sub>2</sub> in a slurry photoreactor, *J. Chem. Technol. Biotechnol.*, 81 (2006) 365–373.
- [19] S.P. Kamble, S.B. Sawant, V.G. Pangarkar, Batch and continuous photocatalytic degradation of benzenesulfonic acid using concentrated solar radiation, *Ind. Eng. Chem. Res.*, 42 (2003) 6705–6713.
- [20] B. Cojocar, Ș. Neațu, V.I. Pârvulescu, V. Șomoghi, N. Petrea, G. Epure, M. Alvaro, H. Garcia, Synergism of activated carbon and undoped and nitrogen-doped TiO<sub>2</sub> in the photocatalytic degradation of the chemical warfare agents Soman, VX, and Yperite, *Chem. Sus. Chem.*, 2 (2009) 427–436.
- [21] Y. Zhou, S. Zhang, Z. Zhu, Y. Li, Preparation and photocatalytic activity of Gd-doped TiO<sub>2</sub> nanofibre, *J. Cent. South. Univ. T*, 12 (2005) 657–661.
- [22] H.H. Cheng, S.S. Chen, Y.W. Cheng, W.L. Tseng, Y.H. Wang, Liquid-phase non-thermal plasma-prepared N-doped TiO<sub>2</sub> for azo dye degradation with the catalyst separation system by ceramic membranes, *Water Sci. Technol.*, 62 (2010) 1060–1066.
- [23] R.M. Sellers, Spectrophotometric determination of hydrogen peroxide using potassium titanium(IV) oxalate, *Analyst*, 105 (1980) 950–954.
- [24] F. Kiriakidou, D.I. Kondarides, X.E. Verykios, The effect of operational parameters and TiO<sub>2</sub>-doping on the photocatalytic degradation of azo-dyes, *Catal. Today*, 54 (1999) 119–130.
- [25] A. Aleboyeh, H. Aleboyeh, Y. Moussa, “Critical” effect of hydrogen peroxide in photochemical oxidative decolorization of dyes: Acid Orange 8, Acid Blue 74 and Methyl Orange, *Dyes Pigm.*, 57 (2003) 67–75.
- [26] V.L. Snoeyink, D. Jenkins, *Water chemistry*, Wiley (1980), pp. 24–57.
- [27] A.V. Rupa, D. Manikandan, D. Divakar, T. Sivakumar, Effect of deposition of Ag on TiO<sub>2</sub> nanoparticles on the photodegradation of Reactive Yellow-17, *J. Hazard. Mater.*, 147 (2007) 906–913.
- [28] D. Zhao, J. Wang, X. Zhao, J. Zhang, TiO<sub>2</sub>/NaY composite as photocatalyst for degradation of omethoate, *Chem. Res. Chin. Univ.*, 4 (2009) 543–549.
- [29] C.H. Wu, C.H. Yu, Effects of TiO<sub>2</sub> dosage, pH and temperature on decolorization of C.I. Reactive Red 2 in a UV/US/TiO<sub>2</sub> system, *J. Hazard. Mater.*, 169 (2009) 1179–1183.
- [30] P. Bansal, D. Singh, D. Sud, Photocatalytic degradation of azo dye in aqueous TiO<sub>2</sub> suspension: reaction pathway and identification of intermediates products by LC/MS, *Sep. Purif. Technol.*, 72 (2010) 357–365.
- [31] A.V. Rupa, D. Manikandan, D. Divakar, S. Revathi, M.E.L. Preeti, K. Shanthi, T. Sivakumar, Photocatalytic degradation of tartrazine dye using TiO<sub>2</sub> catalyst: salt effect and kinetic studies, *Indian J. Chem. Technol.*, 14 (2007) 71–78.
- [32] W.Y. Wang, Y. Ku, Effect of solution pH on the adsorption and photocatalytic reaction behaviors of dyes using TiO<sub>2</sub> and Nafion-coated TiO<sub>2</sub>, *Colloids Surf. A-Physicochem. Eng. Asp.*, 302 (2007) 261–268.
- [33] M. Zhang, T. An, J. Fu, G. Sheng, X. Wang, X. Hu, X. Ding, Photocatalytic degradation of mixed gaseous carbonyl compounds at low level on adsorptive TiO<sub>2</sub>/SiO<sub>2</sub> photocatalyst using a fluidized bed reactor, *Chemosphere*, 64 (2006) 423–431.
- [34] T.K. Tseng, Y.S. Lin, Y.J. Chen, H. Chu, A review of photocatalysts prepared by sol-gel method for VOCs removal, *Int. J. Mol. Sci.*, 11 (2010) 2336–2361.
- [35] V. Mirkhani, S. Tangestaninejad, M. Moghadam, M.H. Habibi, A. Rostami-Vartooni, Photocatalytic degradation of azo dyes catalyzed by Ag doped TiO<sub>2</sub> photocatalyst, *J. Iran. Chem. Soc.*, 6 (2009) 578–587.
- [36] X. Zhang, D.D. Sun, G. Li, Y. Wang, Investigation of the roles of active oxygen species in photodegradation of azo dye AO7 in TiO<sub>2</sub> photocatalysis illuminated by microwave electrodeless lamp, *J. Photochem. Photobiol. A Chem.*, 199 (2008) 311–315.
- [37] N.M. Mahmoodi, M. Arami, N.Y. Limaee, N.S. Tabrizi, Kinetics of heterogeneous photocatalytic degradation of reactive dyes in an immobilized TiO<sub>2</sub> photocatalytic reactor, *Curr. Opin. Colloid Interface Sci.*, 295 (2006) 159–164.
- [38] M.A. Rauf, M.A. Meetani, S. Hisaindee, An overview on the photocatalytic degradation of azo dyes in the presence of TiO<sub>2</sub> doped with selective transition metals, *Desalination*, 276 (2011) 13–27.
- [39] J. Sun, L. Qiao, S. Sun, G. Wang, Photocatalytic degradation of Orange G on nitrogen-doped TiO<sub>2</sub> catalysts under visible light and sunlight irradiation, *J. Hazard. Mater.*, 155 (2008) 312–319.
- [40] Y. Liu, X. Chen, J. Li, C. Burda, Photocatalytic degradation of azo dyes by nitrogen-doped TiO<sub>2</sub> nanocatalysts, *Chemosphere*, 61 (2005) 11–18.
- [41] D.E. Gu, B.C. Yang, Y.D. Hu, V and N co-doped nanocrystal anatase TiO<sub>2</sub> photocatalysts with enhanced photocatalytic activity under visible light irradiation, *Catal. Commun.*, 9 (2008) 1472–1476.
- [42] V. Sukharev, R. Kershaw, Concerning the role of oxygen in photocatalytic decomposition of salicylic acid in water, *J. Photochem. Photobiol. A Chem.*, 98 (1996) 165–169.
- [43] P. Borker, A.V. Salker, Photocatalytic degradation of textile azo dye over Ce<sub>1-x</sub>Sn<sub>x</sub>O<sub>2</sub> series, *Mater. Sci. Eng. B Solid State Mater. Adv. Technol.*, 133 (2006) 55–60.
- [44] S. Kaur, V. Singh, TiO<sub>2</sub> mediated photocatalytic degradation studies of Reactive Red 198 by UV irradiation, *J. Hazard. Mater.*, 141 (2007) 230–236.